Nuclear Energy Levels of Na^{24} in the Region from 630 to 860 kev*

CARL T. HIBDON
Argonne National Laboratory, Argonne, Illinois
(Received April 10, 1961)

An investigation of the nuclear level structure of Na^{24} for neutron energies in the range from 630 to 860 kev revealed the presence of 73 levels distributed throughout the range. Each of the two previously known large peaks was found to be composed of a set of levels. These levels are attributable to values of J up to 7 for the first peak and up to $J=6$ for the other one. No s-wave levels were identifiable in this region and it is doubtful that any p-wave levels are present. A set of parameters was determined for the levels by a best fit to the data. These levels were then grouped with those up to 630 kev to obtain a combined total of 230 levels up to 860 kev. The parameters of these levels show the following distributions: (a) an approximate exponential distribution for the level spacings, (b) an approximate exponential or Porter-Thomas distribution for the neutron widths with a tendency to favor the latter, and (c) a distribution of the angular momenta which agrees with the theoretical distribution given by Bloch. Reasonable values of the strength functions were obtained for s- and p-wave levels (0.035 and 0.27, respectively) but the values for $l \geq 2$ appear to be much too large. A plot of the number of levels having energies $\leq E_n$ as a function of E_n shows fluctuations about a linear trend, with no bending away from this trend at high energies to indicate a general missing of levels.

1. INTRODUCTION

RECENTLY, it has been found possible to extend the study of the nuclear energy levels of Na^{24} to higher energies than were reached before and reported in two previous papers, the first of which[1] covered the region up to 350 kev and the second[2] the levels between 350 and 630 kev. These investigations revealed a large number of levels in Na^{24}. This large level density may then be expected to continue on above 630 kev and, if so, the two large peaks reported some years ago by Stelson and Preston[3] in the region between 0.60 and 0.85 Mev should be composed of clusters of narrow levels. The widths of these two peaks appear to be too wide in comparison with the peak heights observed to fit the theory. The reduced widths corresponding to large minimum values of l associated with the large values of J exceed by large factors the sum rule given by Lane *et al.*[4] The existence of clusters of levels of relatively small widths can be revealed if it is possible to attain neutron energy spreads comparable with the spreads used below 630 kev. Initial measurements in the region of the two large peaks show that it is feasible to resolve narrow levels in this region by use of the present neutron counting equipment and techniques described later. The present paper is, then, concerned first with an investigation of the level structure of Na^{24} in the region from 630 to 860 kev, i.e., the type of levels that form the two large clusters. A further concern is a comparison of the distributions of the parameters of all of the levels of Na^{24} up to 860 kev with the predictions given by theory. All energies quoted refer to incident neutron energies in the laboratory system unless otherwise noted.

2. EXPERIMENTAL METHOD

The method of measurement and the techniques used are the same as those used for the study of the resonances in sodium in the region from 350 to 630 kev,[2] and other publications.[1,5] Hence, only a brief outline of the method is given here. The $Li^7(p,n)$ reaction is used to produce nearly monoenergetic neutrons of variable energy. Protons of well-defined energy are produced by the 5-Mev Van de Graaff accelerator. After acceleration, the protons are analyzed by a 17° deflection in a magnetic field and then by a 90° electrostatic analyzer[1] having a radius of 40 in. To define the proton beam, the electrostatic analyzer has entrance and exit slits of 30 and 40 mils wide, respectively. In addition to these vertical slits, a horizontal slit 0.125 in. wide has been placed a few inches before the entrance to the electrostatic analyzer, a second similar slit just before the vertical exit slit, and a third one just ahead of the lithium target assembly. These slits allow very little vertical movement of the proton beam on the lithium target. The proton energies are determined as before[1] by the voltage across the plates of the Argonne precision electrostatic analyzer, which is calibrated by taking the $Li^7(p,n)$ threshold to be 1.881 Mev.

In order to obtain small neutron energy spreads, thin lithium targets are used. These targets are evaporated in vacuum onto the 10-mil tantalum end cap (diameter ≈ 2.7 in.) of the rotating target assembly. During evaporation, the thickness of the lithium is checked at frequent intervals by measuring the yield of neutrons produced by a beam of protons from the accelerator. For this purpose, the proton energy used is close to 2.07 Mev, since the neutron yield is nearly independent of energy in this region. A new target is evaporated daily from lithium metal having an isotopic content purporting to be 99.99% Li^7. The target is cooled by a blast of air. To calibrate the energy and to obtain an estimate of the target thickness, a new rise curve is run daily. All of the present measurements were made by use of neutrons emitted in the direction of the proton beam. The feasibility of measurements in this energy region depends on the capability of the shield to hold the background to an acceptable level and on the neutron energy

* Work performed under the auspices of the U. S. Atomic Energy Commission.
[1] C. T. Hibdon, Phys. Rev. **118**, 514 (1960).
[2] C. T. Hibdon, Phys. Rev. **122**, 1235 (1961).
[3] P. H. Stelson and W. M. Preston, Phys. Rev. **88**, 1354 (1952).
[4] A. M. Lane, R. G. Thomas, and E. P. Wigner, Phys. Rev. **98**, 693 (1955).
[5] C. T. Hibdon, Phys. Rev. **108**, 414 (1957).

spread that can be achieved. The entrance aperture of the collimator through which the neutrons reached the neutron counter had a diameter of 0.3 in. and was located about 11 in. from the source of neutrons. By use of this equipment, it was found that a very good counting rate, with an unexpectedly low background, could be obtained for lithium targets with thicknesses ranging between 0.6 and 0.8 kev. Flat-detection measurements were first made over the entire region by use of a graphite scattering sample, 6 in. long, placed in the counter as shown in Fig. 1 of reference 5. Lucite was used above about 800 kev to obtain a slightly higher counting rate. Measurements made each day overlapped those from the previous day in order to obtain a check on the energy. Only small variations in the energy were encountered. At times, no detectable variations occurred. Some regions were repeated from day to day when slightly thinner lithium targets were deposited. Because of the narrowness of many of the peaks, the entire region was restudied by self-detection in order to resolve the peaks better. For these self-detection measurements, a sodium-scattering sample 0.80 in. thick was used. The same transmission samples of high-purity sodium metal used for the previous measurements up to 630 kev were also used for the present measurements. These samples range in thickness from 0.1 to 3.0 in. and are arranged in sample-containing wheels in such a way that the total thickness can be varied up to 4.5 in. to maintain a transmission of about 50 to 60%. The background was found to be unaffected by these wheels.

The effective over-all neutron energy spread, although estimated by the rise curve at threshold, is still unknown in the present energy region. It is expected to increase with neutron energy but no well-isolated narrow level was found in this region to provide a good indication of the energy spread. However, the degree to which the many overlapping and interfering levels are resolved indicates that the spread is less than might have been expected. The widths of some of the narrowest levels, such as Nos. 158, 160, 177, 191, 201, 217, and the low-energy wing of No. 181 indicate that the effective energy spread is considerably less than 1 kev. The data shown in the various figures are the raw data with no corrections applied other than the following: (1) The data at each energy are normalized by comparison with the count in a BF_3 (enriched to 96% B^{10}) long counter placed 50 in. from the neutron source at an angle of 30° with respect to the direction of the proton beam. (2) A correction is also made for the background, which is obtained by removing the scattering sample from the counting equipment.[5]

3. EXPERIMENTAL RESULTS

The general features of the neutron cross-sectional data in this region are exhibited in several figures in which open circles are used to indicate data obtained by flat detection and solid circles the data by self-detection. Up to 860 kev, the average level spacing of the 231 levels (the 73 levels discussed in this paper plus the 158 below 630 kev, including the bound level at −30 kev) is about 3.9 kev. As suggested by Stelson and Preston,[3] the large peak just above 700 kev is composite. The present results show that a peak in the cluster results from the overlapping of several levels with high values of J. The large peak previously reported near 780 kev[3] consists of a number of relatively wide levels. The large width and high J values of some of these levels result in the formation of a peak in this cluster of levels.

In this region there appear to be no s-wave levels identifiable by their asymmetrical shapes and the presence of deep minima on their low-energy sides. For Na^{24}, the values of J are 1 and 2 for s-wave levels and, in the present energy range, the single-level theoretical peak heights range between 2.4 and 3.5 b (including the potential scattering) for this type of level. The peak heights of the levels which form the two large clusters exceed these values by large factors. Around 750 kev in the region between the two large clusters of levels, the peak heights of the levels are about double the possible heights of s-wave levels. Further, the spacing of these levels is ample to permit one to resolve a deep minimum on the low-energy side of an s-wave level in this region if any exists. The only other region where s-wave levels might be expected is around 850 kev. But here again, the observed peak heights of the levels are about twice the possible heights for s-wave levels and the level spacings are ample to observe any deep minima associated with s-wave levels.

One interesting feature of the data is the distribution of the levels—whether they occur at random or at regular intervals. A knowledge of this distribution is useful both for practical purposes and in connection with the theory of nuclear structure. Figure 1 shows the

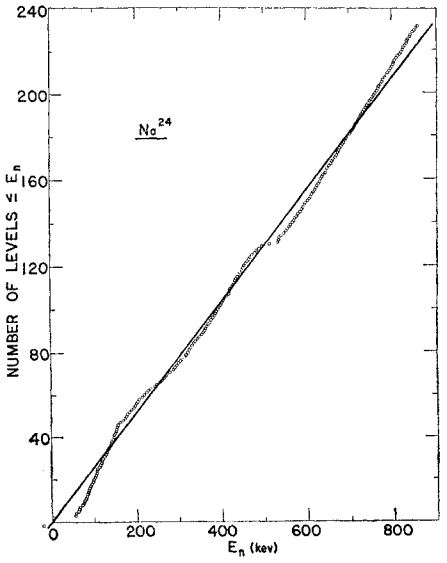

FIG. 1. Number of levels of Na^{24} with energies $\leqslant E_n$ as a function of the neutron energy E_n.

number of levels with energies $\leqslant E_n$ plotted as a function of the neutron energy E_n for all of the levels of Na^{24} up to 860 kev. It was expected that a general missing of levels might set in as one progressed to higher energies because of the increase in the spread in energy of the neutrons. However, the plot in Fig. 1 shows no downward curvature in the high-energy region to indicate a general missing of levels. Instead, the plot shows fluctuations about an almost straight line. These fluctuations, which occur throughout the energy range, presumably are attributable in part to a missing of some very narrow levels and in part to a random occurrence of the levels that would occur for any appropriate model of the nucleus.

In this region, the interactions of the neutrons with sodium are taken to be due primarily to elastic scattering. It was shown, mainly in the second paper[2] of this series, that the competing processes such as (n,p), (n,α), and (n,γ) are negligible in this region. However, inelastic scattering of neutrons may not be completely negligible between 700 and 800 kev, where the highest value[2,6] of the inelastic scattering cross section is about 300 mb. The peaks (Fig. 2 of reference 6) in the inelastic scattering cross section correspond to the peaks of the clusters in the present measurements and show widths comparable with the widths of the clusters. Undoubtedly the inelastic scattering is, then, distributed among the many small peaks of the clusters and not localized in a few. Thus it appears that the inelastic scattering process may be omitted in the present analyses.

Prominent peaks of Na^{24} in the low-energy region may be reflected as spurious peaks at higher energies because the neutron beam from the lithium target contains a second group of low-energy neutrons that arises from the formation of the residual nucleus Be^7 in the 430-kev excited state.[1] However, in the present measurements, these spurious peaks can occur only in the region above about 640 kev. Then the first levels (Nos. 42 and 43)[1] that are likely to cause spurious peaks are located at about 205 kev and would be expected to show

TABLE I. Summary of the levels of Na^{24} (from 630 to 860 kev) derived from neutron reactions with Na^{23}. The parameters J, Γ, and l are probable values obtained as a best fit to the data. The sample thickness used for self-detection measurements at the peaks of the levels is given by N_s. The sample thickness for flat detection is the same as N_s for the wide levels and up to 50% more for the narrow ones.

No.	E_r (kev)	J	l	Γ_n (kev)	N_s (10^{24} atoms/cm^2)	No.	E_r (kev)	J	l	Γ_n (kev)	N_s (10^{24} atoms/cm^2)
138	629.8	3	2	1.80	0.0956	175	747.0	3	2	2.50	0.1279
139	632.9	2	3	1.00	0.0956	176	749.8	2	2	2.60	0.1279
140	634.8	2	3	1.20	0.0956	177	752.4	1	2	2.20	0.1279
141	638.0	3	2	2.20	0.0956	178	756.3	3	2	3.40	0.1279
142	642.2	2	3	1.70	0.0956	179	759.8	1	2	1.90	0.1279
143	645.1	2	3	1.40	0.0956	180	763.4	3	2	2.00	0.1279
144	647.9	3	3	1.20	0.0956	181	766.7	5	4	1.80	0.0956
145	651.5	3	3	1.90	0.1279	182	768.6	3	2	1.90	0.0956
146	655.6	3	2	2.30	0.0956	183	773.3	5	3	3.20	0.0956
147	658.1	3	3	1.60	0.0956	183A	776.0	1	2	1.30	
148	661.4	3	2	2.30	0.0956	184	778.2	5	3	2.90	0.0956
149	665.8	4	2	2.00	0.0956	185	782.4	3	2	3.60	0.0956
150	669.3	2	2	2.40	0.0956	186	786.3	6	4	2.60	0.0956
151	672.0	3	2	1.80	0.0956	186A	789.2	1	2	2.10	
152	674.1	2	2	2.80	0.0956	187	792.4	5	3	2.90	0.0956
153	676.6	3	2	2.60	0.0956	188	795.8	5	4	2.10	0.0956
154	679.7	2	2	2.10	0.0956	189	798.7	5	3	2.40	0.0956
155	682.4	4	3	1.70	0.0956	190	801.0	3	2	2.00	0.0956
156	685.6	6	4	1.90	0.0639	190A	802.7	1	2	2.10	
157	688.8	6	4	1.70	0.0639	191	806.9	4	2	3.40	0.0956
158	692.4	5	4	2.60	0.0639	191A	809.0	1	2	2.20	
159	696.5	4	2	3.40	0.0639	192	812.6	4	2	4.00	0.0956
160	700.3	5	3	4.10	0.0639	193	818.0	2	3	2.00	0.0956
161	703.3	4	2	2.50	0.0639	194	821.0	4	3	2.00	0.0956
162	707.3	6	4	1.80	0.0639	195	824.0	3	3	2.00	0.1279
163	709.5	6	5	1.60	0.0639	196	826.4	2	3	2.20	0.1279
164	712.1	6	4	2.40	0.0639	197	830.1	4	3	2.10	0.1279
165	716.0	7	5	3.00	0.0639	198	832.5	3	3	1.50	0.1279
166	719.3	4	3	2.30	0.0639	199	835.0	2	2	2.30	0.1279
167	721.6	6	5	2.20	0.0639	200	836.8	2	3	1.50	0.1279
168	724.8	6	4	2.70	0.0639	201	841.2	3	3	2.20	0.1279
169	727.9	4	3	2.70	0.0639	202	843.8	4	3	1.70	0.1279
170	731.0	6	4	2.10	0.0639	203	847.7	3	3	2.30	0.1279
171	734.0	6	5	1.70	0.0956	204	852.0	2	2	2.80	0.1598
172	736.8	4	2	2.50	0.0956	205	854.5	1	2	2.60	0.1598
173	740.5	5	3	3.00	0.0956	206	857.5	2	2	3.00	0.1598
174	744.2	2	2	2.50	0.0956						

[6] R. O. Lane and J. E. Monahan, Phys. Rev. **118**, 533 (1960), Fig. 2.

spurious peaks near 742 kev, but no discernible peak occurs at this energy. When the main group of neutrons has an energy of 770 kev, the low-energy component has an energy of 242 kev. Therefore, the 242-kev resonance, the widest level revealed in Na^{24} by the present study, might be expected to re-appear as a spurious peak at 770 kev, but no detectable peak occurs at this energy. The only other possibility is the s-wave level at 302.5 kev[1] but no corresponding spurious peak occurs at 820 kev. All other peaks appear to be too small to produce detectable spurious peaks. One cannot unambiguously rule out the possibility of spurious peaks due to the second group of neutrons at the higher values of the energies. However, a shift of at least 2 kev would be necessary for the spurious peaks to coincide with observed peaks, but these peaks are too large to be accounted for by the expected fractions[7] of low-energy neutrons. For the present work, these fractions appear to amount to no more than about 2.5%.[7] Spurious peaks would hardly be distinguishable, then, in the presence of so many peaks in Na^{24}.

4. ANALYSES OF THE RESONANCE LEVELS

It is desirable to know something about the nature of the levels that form the two large clusters and the levels in the wings of these clusters. Therefore, an attempt has been made to determine what variety of levels would account for the behavior of the data, i.e., to determine a set of parameters of the many levels that provide a best fit to the data and that give a reasonable account of the peak heights. The large level density and the consequent narrow spacings with overlapping and interfering wings of the levels prevent one from resolving the levels well enough to lead to an accurate determination of the parameters of the levels. However, it was found that the levels are sensitive to the widths used and neighboring levels become distorted in shape when the widths of one or two levels are varied appreciably. Therefore, a set of parameters of the many levels that account for the data has been determined and is given in Table I. The method of analysis is outlined later but first a value of the potential scattering σ_p that is reasonably close to the true value must be known. This value cannot be determined directly from the present data because there is no region free of the wings of the many levels nor is there an s-wave level whose minimum would provide some indication of the value of the potential scattering. For reasons presented in the two preceding papers,[1,2] the value of σ_p is taken to be given by

$$\sigma_p=\sum_l(2l+1)4\pi\lambda\!\!\!^{-2}\sin^2\delta_l.$$

The method of analysis is the same as that used in the region below 630 kev.[1,2] For some levels, estimated parameters were used to obtain single-level plots which approximately fit the data. The parameters were repeatedly revised until a best fit to the data was obtained. Because of the density of levels, many single-level and multiple-level plots were considered simultaneously in order to take into account the effects of overlapping and interfering wings of a group or groups of levels. The plots which provide the best fit to the data are shown in the appropriate figures. It is usually more convenient to begin the analyses with the s-wave levels. However, no s-wave levels are recognizable in the present data, but the wings of the s-wave levels at lower energies extend into this region. Their multiple-level contribution plus the potential scattering is shown along with the data by curve A in Figs. 2–6. This curve is a little above the

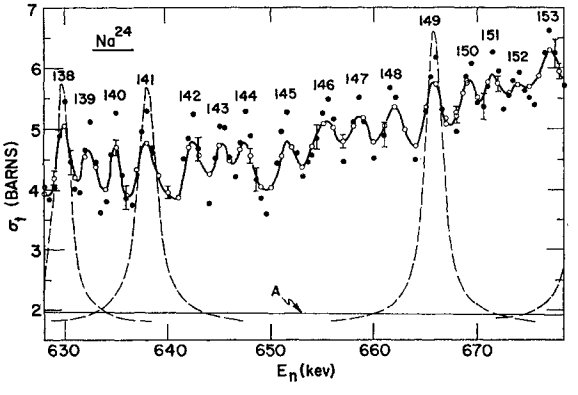

FIG. 2. Neutron total cross section of sodium from 628 to 680 kev. Open circles show data obtained by flat detection; solid circles data by self-detection. Curve A is a multiple-level plot of the s-wave levels that extend into this region. It includes the potential scattering. Other curves shown by broken lines are theoretical plots for the best fits of the appropriate levels.

[7] A. B. Smith (private communication).

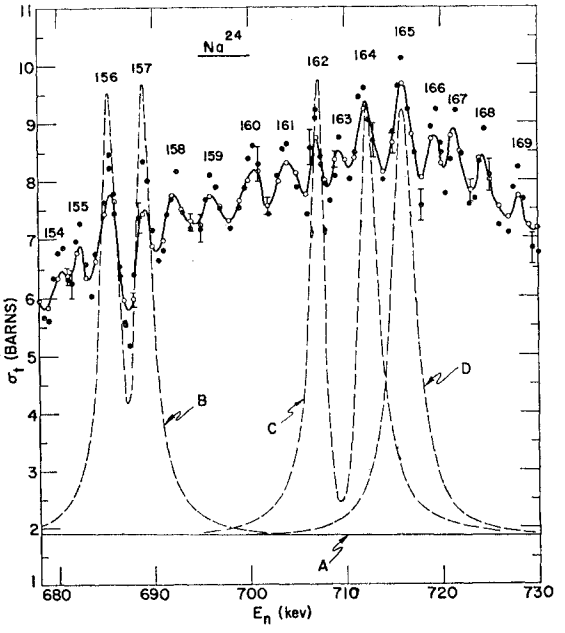

FIG. 3. Neutron total cross section of sodium from 678 to 730 kev. Open circles show data obtained by flat detection; solid circles data by self-detection. Curve A shows a multiple-level plot of the s-wave levels that extend into this region. It includes the potential scattering. Curves B, C, and D are theoretical plots for the best fits obtained for the appropriate levels.

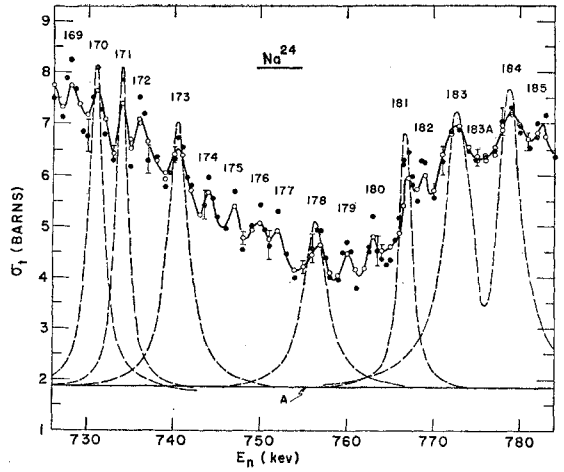

FIG. 4. Neutron total cross section of sodium from 726 to 784 kev in the region between the two clusters of peaks having large values of J. Open circles show data obtained by flat detection; solid circles data by self-detection. Curve A shows the multiple-level plot of the s-wave levels that extend into this region. Other curves shown by broken lines represent the best fits obtained for the appropriate levels.

potential scattering and provides the background upon which the levels of this region sit. The many tedious calculations needed were performed by the Applied Mathematics Division on the IBM-704 computer. The values of the parameters given in Table I are the ones for which the computer program gave the best fit to the experimental points as determined by a visual comparison. The equations on which the program is based are given in reference 8, p. 182. Equation (2) is used for multiple-level plots and Eq. (3) for single-level plots. The variation of the width Γ_n with energy is included in accordance with $\Gamma_n=2P_l\gamma_l^2$ so that the wings of the levels may be extended as far as required. The factor P_l is the penetrability factor given by $P_0=x$, $P_1=x^3/(x^2+1)$, etc., with $x=R/\lambda$. A method is under study for correlating the data obtained by flat- and self-detection and the neutron energy spread in an effort to obtain an analytical determination of the correct value of J for narrow levels. The method is quite involved and when completed will be given in a separate paper. An approximate form which is valid at the peaks of levels, has been applied to the narrow levels of this region and agrees with the J-value assignments. In applying this method, corrections were made for the wings of neighboring levels.

A. Analyses of the Resonance Levels from 630 to 760 kev

The peaks observed during the present measurements can be conveniently divided into two groups: (1) The first group comprises the peaks from 630 to about 760 kev, i.e., the region centering around the first cluster of high peaks, and (2) the second group includes the cluster of high peaks from 760 to 860 kev. Consider first the region from 630 to 760 kev, which is shown in Figs. 2–4. This region shows a trend toward high values of J, and in the neighborhood of the peak of the first cluster, which is just below 700 kev, some of the highest values of J occur for Na^{24}. Figure 2 shows the region of the low-energy wing of this first cluster of high peaks. The theoretical curve for peak No. 138 shown by a broken line was obtained for a value of $J=3$ and a width of 1.80 kev ($l=2$). A value of $J=3$ can be assigned to No. 141. The curve shown for this level was obtained for a width of 2.20 kev ($l=2$). The curve shown for No. 149 was obtained by use of the parameters $J=4$, $\Gamma_n=2.00$ kev, and $l=2$. These three peaks were chosen

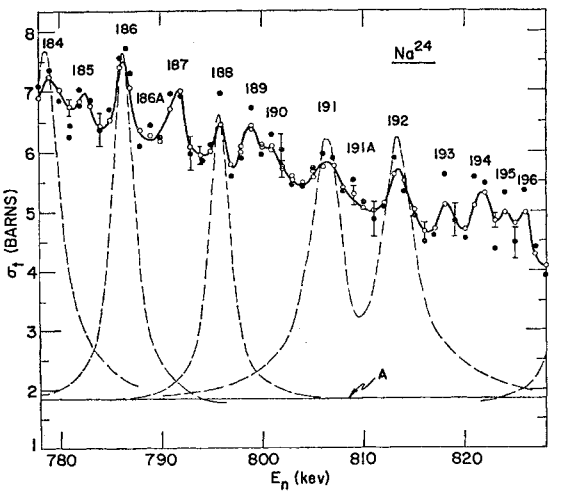

FIG. 5. Neutron total cross section of sodium from 778 to 828 kev. Open circles show data obtained by flat detection; solid circles data by self-detection. Curve A shows the multiple-level plot of s-wave levels that extend into this region. Other curves shown by broken lines represent the best fits obtained for the appropriate levels.

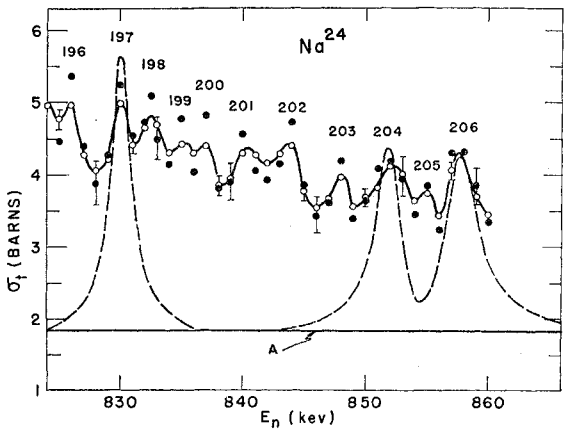

FIG. 6. Neutron total cross section of sodium from 824 to 860 kev. Open circles show data obtained by flat detection; solid circles data by self-detection. Curve A shows a multiple-level plot of the s-wave levels that extend into this region plus potential scattering. Plots for the best fits to peaks Nos. 197, 204, and 206 are shown by broken lines.

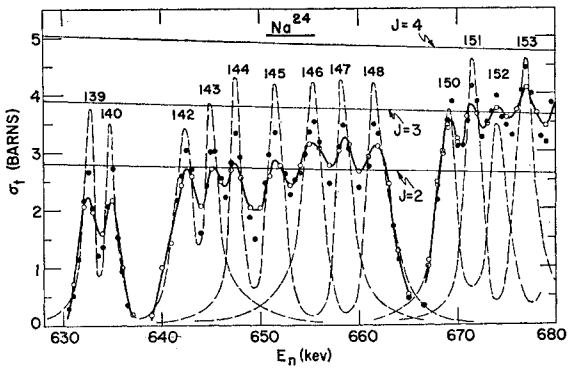

FIG. 7. Analyses of the levels of Na^{24} from 628 to 680 kev. The points shown were obtained by subtracting the broken curves in Fig. 2. Curves shown by broken lines are theoretical plots obtained by use of the parameters given in Table I. The lines showing possible peak heights are for single-level peak heights for $l \geq 1$. No curve includes the potential scattering.

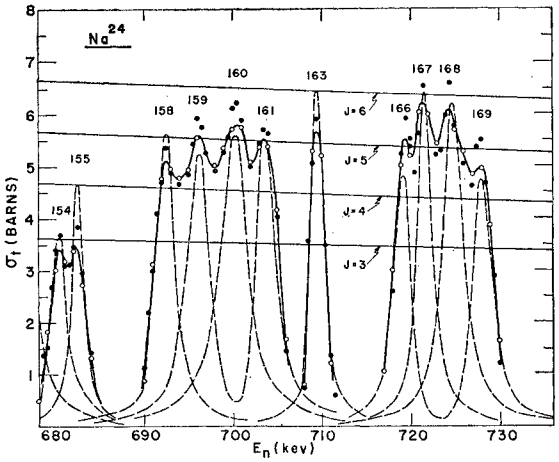

FIG. 8. Analyses of the levels of Na^{24} from 678 to 730 kev. The points shown were obtained by subtracting the dashed curves in Fig. 3. Theoretical plots for the best fits are shown by broken lines. Possible single-level peak heights for various values of J are shown by solid lines for $l \geq 1$. No curve includes the potential scattering.

first because their peak heights appear to be the least affected by nearby levels and their wings are as well defined as the wings of any of the peaks. By subtracting the resonance contributions of these three levels and curve A from the data in Fig. 2, one obtains the curves shown by solid lines in Fig. 7. The self-detection data indicate a range in the values of J from 2 to 4 for the levels in Fig. 7. Relatively deep valleys occur between peaks Nos. 139 and 140 and between 142 and 143. The multiple-level plot shown is for a value of $J=2$ for the widths given in Table I. The following noticeable features are useful aids in determining the parameters of the next five peaks, Nos. 144–148: (1) the value of J appears to be 3 for all of these peaks, (2) a deep minimum between Nos. 144 and 145 denotes mutual interference, (3) no deep minimum occurs between any other pair of adjacent peaks, and (4) the widths of Nos. 146 and 148 are larger than the widths of the remaining three peaks. Hence, a smaller value of l must be assigned to these latter two peaks than to the other three. The depths of the minima are insufficient to confirm mutual interference between adjacent pairs of peaks Nos. 145 through 148. Therefore, two multiple-level plots can account for these five peaks: (1) a multiple-level plot for Nos. 144, 145, and 147, and (2) a multiple-level plot for Nos. 146 and 148. These plots, shown in Fig. 7, were obtained by use of the parameters given in Table I. The next group beginning with No. 150 must include the levels through No. 155. However, one must also take into account the extensive low-energy wings of the pair of levels Nos. 156 and 157 shown in Fig. 3. Then, in Figs. 7 and 8, the group comprising Nos. 150–155 exhibits the following features: (1) the levels are somewhat more closely spaced than in the previous group, and this produces a strong overlapping of the many wings, (2) no deep minima occur between the peaks, and (3) apparently the widths of these peaks do not differ by a large amount. Because of the strong overlapping of the wings and the lack of any apparent mutual interference between adjacent levels, it is more difficult to assign values of J. However, by trial and error, it was found that the following scheme provides the best approach: assign (1) a value of $J=2$ to Nos. 150, 152, and 154 for a value of $l=2$, (2) a value of $J=3$ to Nos. 151 and 153 for $l=2$, and (3) a value of $J=4$ to No. 155 for $l=3$. The theoretical plots shown in Figs. 7 and 8 were obtained from the values of J and the widths given in Table I.

The data in Fig. 3 show a cluster of high peaks which exhibits the largest values of J observed in Na^{24}. The degree to which these peaks are resolved indicates a strong overlapping of the many wings and, from the number of peaks, one sees that the average width of the levels is of the order of 3.0 kev or less. Only one pair of adjacent peaks, Nos. 156 and 157, shows a relatively deep intervening minimum. Apparently, the overlapping wings of neighboring levels contribute very little to the peak heights of these two levels. Therefore, their parameters were estimated and then adjusted until a reasonably good fit to the data was obtained. A multiple-level plot is shown by curve B in Fig. 3 for a value of $J=6$ for widths of 1.90 and 1.70 kev, respectively, for Nos. 156 and 157. It is to be noted that the minimum value of l is 4 for a value of $J=6$. The corresponding reduced widths are, then, extremely large. The parameters for Nos. 162, 164, and 165 were also determined by trial and error. The multiple-level plot shown by curve C was computed for $J=6$ for the widths shown in Table I. The observed height of peak No. 165 is a little above the corresponding theoretical single-level height for $J=7$ but below the value for $J=8$. A level of this apparent width is expected to be almost completely resolved to its true height. However, the observed height appears to exceed the true height because wings of nearby levels elevate the peak of No. 165 considerably and, when these wings are taken into account, the

height will be reduced by about 1 to 1.5 b. Therefore, the value of J is taken to be 7. Curve D in Fig. 3 shows a single-level plot for a width of 3.0 kev. For a value of $J=7$, the minimum value of l is 5, and this leads to an excessively large reduced width for a neutron width of 3.0 kev.

Curves shown by solid lines in Fig. 8 were obtained by subtracting curve A and the resonance components of curves B, C, and D from the data in Fig. 3. No deep minima occur between successive peaks in the group Nos. 158–161 to indicate mutual interference. Either these levels are narrow and the valleys between them poorly resolved or the widths are sufficiently large that the overlapping wings of the levels elevate the valleys to such an extent that one can expect to resolve them very little more even by use of neutrons of smaller energy spreads. The spacings of these levels are comparable with the spacing between Nos. 156 and 157 where a deep valley was resolved. Therefore, one expects relatively large widths for the four levels under consideration and correspondingly shallow valleys between the levels. Because of these widths, one expects that the observed heights of these peaks are near the true heights. Possibly the peaks of Nos. 158 and 161 could be increased by small amounts by use of neutrons of smaller energy spreads. The overlapping wings elevate these peaks above their true heights and this must be considered. The amount of these contributions can be determined by simultaneous consideration of the plots of all these levels. These plots are shown in Fig. 8. A single-level plot is shown for No. 158 for $J=5$ and a width of 2.60 kev ($l=4$) and for No. 160 for $J=5$ and a width of 4.10 kev ($l=3$). The multiple-level plot for Nos. 159 and 161 was computed for widths of 3.40 and 2.50 kev, respectively, for $J=4$ ($l=2$).

A single-level plot is shown in Fig. 8 for peak No. 163 for a value of $J=6$ and $\Gamma_n=1.70$ kev. No mutual interference with Nos. 162 and 164 is indicated by the depths of the minima. Therefore, a larger value of l is assigned to No. 163 than to Nos. 162 and 164. The last group of levels in Fig. 8 can be accounted for by $J=4$ for Nos. 166 and 169 with widths of 2.30 and 2.70 kev, respectively, and $J=6$ for Nos. 167 and 168 with widths of 2.20 and 2.70 kev, respectively. A multiple-level plot is shown for Nos. 166 and 169 and single-level plots for the other two levels.

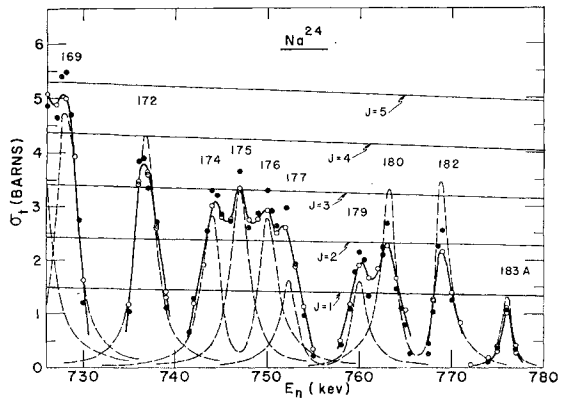

FIG. 9. Analyses of the levels of Na^{24} from 726 to 780 kev. Points shown were obtained by subtracting the broken curves in Fig. 4. Plots for the best fits are drawn as broken lines. Possible single-level peak heights are shown by solid lines for $l \geq 1$. No curve includes the potential scattering.

The data for the remainder of the levels in the range from 630 to 760 kev are shown in Fig. 4. Mutual interference between adjacent pairs of levels is not immediately recognizable because there are no deep minima between the levels to indicate it. By trial and error a set of parameters was determined for Nos. 170, 171, 173, and 178. These parameters are listed in Table I and the plots obtained with them are shown in Fig. 4. By subtracting curve A and the resonance part of these plots from the data, one obtains the curves shown by solid lines in Fig. 9. The plot shown for No. 172 was obtained by the parameters $J=4$ and $\Gamma_n=2.50$ kev ($l=2$). It was found that levels Nos. 174 and 176 ($l=2$) could be attributed to $J=2$, No. 175 to $J=3$, and Nos. 177 and 179 to $J=1$. The plots shown in Fig. 9 were obtained by use of the widths shown in Table I. These plots give a reasonable account of the data when the contributions of the overlapping wings are taken into account.

B. Analyses of the Resonance Levels from 760 to 860 kev

Part of the data for the second group of levels is shown in Fig. 4 and the remainder in Figs. 5 and 6. The region centered around 780 kev comprises a cluster of peaks with high values of J. Some levels in the cluster have relatively large widths. A number of fairly wide levels also occur in other parts of the region outside of the cluster of high peaks. No minima anywhere in the data shown in Figs. 4–6 are sufficiently deep between the levels to enable one to recognize mutual interference between adjacent pairs of levels by inspection. In Fig. 4, one sees that the low-energy wing of No. 181 is sufficiently revealed to obtain an estimate of its width. The peak height indicates a value of $J=5$. However, this value of J may be too large because the wings of neighboring levels, especially Nos. 183 and 184, may elevate the peak of No. 181 to such an extent that a value of $J=4$ is applicable. Because of their relatively large widths, Nos. 183 and 184 appear to be resolved to their true peak heights, which correspond to a value of $J=5$. There appears to be no way to determine the widths of these two peaks other than by trial and error, which involves a considerable amount of revision of the parameters. Their widths and heights are approximately equal and this indicates mutual interference. However, the valley between them is far too shallow to confirm mutual interference, and one would expect to resolve it to a much lower value unless another peak is located in the valley. For either a single- or multiple-level analysis,

a third peak No. 183A always appears between Nos. 183 and 184. Therefore, a multiple-level plot for Nos. 183 and 184 best accounts for the data. The plot shown in Fig. 4 is for $J=5$ and the widths shown in Table I. One sees, then, that the peak of No. 181 is not sufficiently affected by the wings of Nos. 183 and 184 to assign a value of $J=4$. Therefore, a single-level plot is shown in Fig. 4 for $J=5$ and $\Gamma_n=1.80$ kev ($l=4$). By subtracting curve A and the resonance contributions of Nos. 181, 183, and 184 from the data, one obtains the curves shown in Figs. 9 and 10. The peak heights and widths of Nos. 180 and 182 appear to be comparable. Therefore, a multiple-level plot shown in Fig. 9 for $J=3$ ($l=2$) and $\Gamma_n=2.00$ and 1.90 kev, respectively, appears to agree with the data. A single-level plot is shown for No. 183A for $J=1$ and a width of 1.30 kev ($l=2$).

Figure 5 shows the high-energy side of the cluster of high peaks. No deep minima occur between the peaks. There are a number of widely spaced levels and one would expect to see deeper minima between them than was observed, but the data indicate the presence of small peaks in these valleys. Peak No. 186 appears to be sufficiently removed from neighboring peaks to obtain the value of J directly from the data. Its height is slightly above the corresponding height for a value of $J=6$ but well below the corresponding value for $J=7$. No significant increase in height was obtained by self-detection. Therefore, the value of J is taken to be 6. The single-level plot shown by a broken line in Fig. 5 was obtained for a width of 2.60 kev. The minimum value of l is 4.

Peaks Nos. 187, 188, and 189 exhibit nearly equal heights, which slightly exceed the corresponding single-level peak heights for $J=5$. Apparently, no mutual interference occurs between adjacent pairs of these levels because no deep valleys were observed between them, but this does not rule out the possibility of mutual interference between Nos. 187 and 189. Moreover, the wings of adjacent levels elevate the peaks of Nos. 187 and 189 somewhat but No. 188 is too far removed to be affected appreciably by them. The amount of the elevation of Nos. 187 and 189 appears to be sufficient to indicate a value of $J=4$ for these two peaks, in which case mutual interference may be expected. Then the peak height of No. 188 is little affected by the wings of 187 and 189 because it is located near the minimum between these two peaks. By trial and error, it was found that this approach produced the best results. Therefore, the single-level plot for No. 188, Fig. 5, is drawn for $J=5$, $\Gamma_n=2.40$ kev, $l=4$. Numbers 191 and 192 are the widest levels in this region and appear to be well resolved. Their peak heights correspond to the single-level theoretical peak height for $J=4$. One, then, expects mutual interference between these two levels. However, variations in the valley between these two peaks indicate the presence of a small peak, No. 191A, which prevents one from observing a deep valley

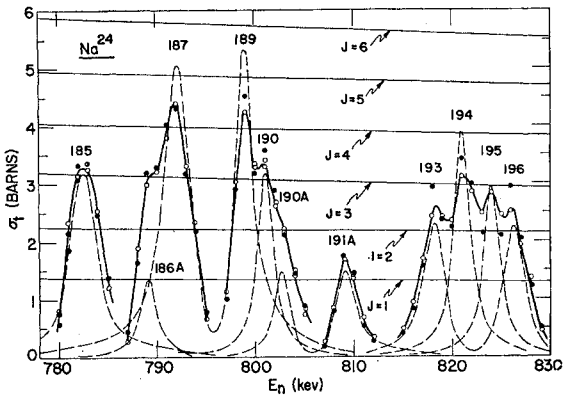

FIG. 10. Analyses of the levels of Na^{24} from 778 to 830 kev. Points shown were obtained by the subtractions made in Fig. 5. Plots for the best fits are shown as broken lines. Possible single-level peak heights are shown by solid lines for $l\geq 1$. No curve includes the potential scattering.

attributable to mutual interference. A multiple-level plot for Nos. 191 and 192 provides the best agreement with the data. This plot is shown in Fig. 5 for $J=4$ and the widths listed in Table I for $l=2$, which is the minimum value of l. By subtracting the resonance contributions of Nos. 186, 188, 191, and 192 plus curve A from the data in Fig. 5, one obtains the curves shown by solid lines in Fig. 10. The single-level plot shown for peak No. 185 was obtained for $J=3$ with a width of 3.60 kev ($l=2$), which, together with the wings of other nearby levels, accounts for this peak. The multiple-level plot for Nos. 187 and 189 is shown in Fig. 10 for $J=5$ ($l=3$) and the widths listed in Table I. Peak No. 190 appears to be attributable to $J=3$ and the single-level plot shown was obtained for a width of 2.00 kev. The residual peaks Nos. 186A, 190A, and 191A appear to be attributable to $J=1$ and the plot shown was obtained by use of the widths given in Table I. The following plots account for the group of peaks Nos. 193–196: (1) a multiple-level plot for Nos. 193 and 196 for a value of $J=2$, (2) a single-level plot for No. 194 for a value of $J=4$, and (3) a single-level plot for No. 195 for a value of $J=3$. The remaining parameters are given in Table I.

The remaining data are shown in Fig. 6. Peak No. 197 rises to a height just below the height corresponding to $J=4$. Wings of nearby narrow levels do not appear to affect this peak sufficiently to make $J=3$ a preferable assignment. Therefore a single-level plot is shown for $J=4$ and a width of 2.10 kev ($l=3$). A multiple-level plot is shown for Nos. 204 and 206 for $J=2$ and widths of 2.80 and 3.00 kev, respectively. By subtracting the resonance contributions of Nos. 197, 204, and 206 plus curve A from the data in Fig. 6, one obtains the curves shown in Fig. 11. By trial and error, it was found that the following assignments account for these peaks: (1) a single-level plot for No. 198 for $J=3$, (2) single-level plots for Nos. 199 and 200 for $J=2$, (3) a multiple-level

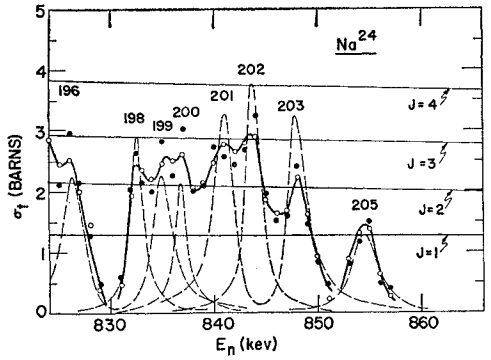

FIG. 11. Analyses of the levels of Na^{24} from 824 to 860 kev. Points shown were obtained by subtracting the dashed curves in Fig. 6. Plots for the best fits are shown as broken lines. Possible single-level peak heights for a number of values of J are shown by solid lines for $l \geq 1$. No curve contains the potential scattering.

plot for Nos. 201 and 203 for $J=3$, (4) a single-level plot for No. 202 for a value of $J=4$, and (5) a single-level plot for No. 205 for $J=1$. The widths are given in Table I.

A total of 73 levels were observed in this region and, when combined with the levels[1,2] observed up to 630 kev and the bound level at -30 kev, amount to 231 levels up to 860 kev. Table I gives a summary of the parameters of the 73 levels in this region as determined by the analyses. Table II gives the number of levels assigned to each value of J for all levels of Na^{24} up to 860 kev and their distribution among the various values of J. The parameters given in these tables are those that appear to give a best fit to the data. There appears to be no means by which one can distinguish clearly between values of l for $l>0$. One might expect a sizable number of levels to be attributable to p-wave neutron interactions. But, if the values of the reduced widths are taken to be meaningful, p-wave levels are unlikely because the largest neutron width observed, 4.10 kev, corresponds to a reduced width of less than 8.9 kev for this type of level. On the other hand, many levels are attributable to high values of J corresponding to large values of l and hence to excessively large reduced widths. Possible values of J were computed by the method[8] used for the levels of Al^{28}. Then, if one invokes the Wigner limit[8] and attempts to compare the reduced widths with this limit, it is found that many reduced widths exceed this limit by large factors. For the neutron widths found, these large reduced widths are inescapable. Then, unless it can be shown that these peaks, assignable to high values of J and l, consist of a number of very narrow levels, the Wigner limit serves no purpose. Possibly, this limit is really valid only for s- and p-wave levels at low energies. Still, no analyses can be performed unless some value of l is assigned. Therefore, the lowest values of l consistent with the data were assigned. This produces some inconsistencies because of the high values of l associated with some values of J and because of assignments made in keeping with the presence or absence of evidence for mutual interference. The peak heights, widths of levels, and depths of valleys between peaks do provide strong arguments for various values of l. In principle, angular distribution measurements could aid in determining better values of l. However, in the presence of so many overlapping and interfering wings of the levels, clear conclusions could hardly be anticipated. Further, acceptable counting rates for the small neutron energy spreads needed may prove difficult to obtain.

[8] C. T. Hibdon, Phys. Rev. **114**, 179 (1959).

5. DISTRIBUTIONS OF THE PARAMETERS OF THE LEVELS

It is desirable to compare the distributions of the parameters of the levels with the predictions of nuclear theory. Because of the large density of levels and the consequent overlapping of wings of levels and the generally narrow widths of levels, many of the levels cannot be resolved sufficiently to determine their parameters accurately. The parameters determined represent values obtained by a best fit to the data. Therefore, these parameters may be sufficiently inaccurate to introduce irregularities into the distributions. Nevertheless, the comparisons are made on the basis of the parameters that have been determined. All of the levels of Na^{24} up to 860 kev are included. (See references **1** and 2 for tabulations of the levels up to 630 kev.) Only the values of the parameters obtained in the analyses were used; no corrections were applied for neutron energy spread, nor have any corrections been attempted to take account of missed levels.

A. Neutron Widths

The reduced widths of the levels, obtained from the neutron widths by the relation[8] $\gamma_l^2=\Gamma_n/(2P_l)$, were found to fluctuate violently among the levels of Na^{24}. Several years ago Scott[9] proposed that the distribution of reduced widths is exponential. A first study by Harvey *et al.*[10] and by Hughes and Harvey[11] with low-energy neutrons showed that the distribution is roughly exponential in form. Porter and Thomas[12] assumed that

TABLE II. Distribution of the angular momentum J among the levels of Na^{24}. The relative numbers are the ratios of the densities of levels to the density for $J=1$. All resonance levels of Na^{24} up to 860 kev are included.

J	0	1	2	3	4	5	6	7
Number of levels	27	54	60	45	24	9	10	1
Relative numbers	0.50	1.00	1.11	0.83	0.44	0.17	0.18	0.02

[9] J. M. C. Scott, Phil. Mag. **45**, 1322 (1954).
[10] J. A. Harvey, D. J. Hughes, R. S. Carter, and V. E. Pilcher, Phys. Rev. **99**, 10 (1955).
[11] D. J. Hughes and J. A. Harvey, Phys. Rev. **99**, 1032 (1955).
[12] C. E. Porter and R. G. Thomas, Phys. Rev. **104**, 483 (1956).

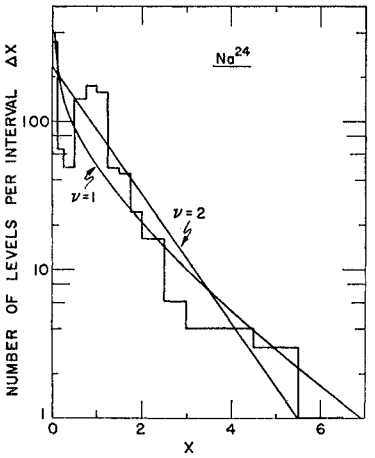

FIG. 12. Distribution of the reduced neutron widths of Na^{24}. The histogram shows the experimental data for all known virtual levels up to 860 kev. For $\nu=2$, the resulting exponential curve is for $C=230$ in Eq. (1). The curve for $\nu=1$ shows the Porter-Thomas distribution for $81\,x^{-\frac{1}{2}}\exp(-\frac{1}{2}x)$.

the correct distribution of the reduced widths is one of the class of χ^2 distributions of the form

$$y=C(\tfrac{1}{2}\nu)^{-1}(\tfrac{1}{2}\nu x)^{\frac{1}{2}\nu-1}e^{-\frac{1}{2}\nu x}, \qquad (1)$$

where $x=\gamma^2/\langle\gamma^2\rangle_{\rm av}$, γ^2, and $\langle\gamma^2\rangle_{\rm av}$ refer to a particular J and parity. The quantity ν refers to the number of degrees of freedom[12] and C is a constant. Then, y represents the number of reduced widths per unit interval Δx. For a value of $\nu=2$, Eq. (1) reduces to the exponential distribution given by Scott.[9] The value $\nu=1$ gives the Porter-Thomas distribution.[12] A further study by Porter and Rosenzweig[13] indicates that the value of $\nu=1$ is at least approximately correct.

The present data for Na^{24} are shown by a histogram in Fig. 12 in which the number of reduced widths per unit interval Δx is plotted against x. To obtain this plot, the reduced widths were first separated into sequences, each belonging to a given J and parity, and the mean spacing was computed separately for each sequence. The several sequences were then combined into a single distribution. For comparison, the theoretical distributions given by Eq. (1) for values of $\nu=1$ and 2 are also shown in Fig. 12. The curve shown for $\nu=1$ was obtained from the expression $81x^{-\frac{1}{2}}\exp(-\frac{1}{2}x)$ and the curve for $\nu=2$ from the expression $230\exp(-x)$. The data represented by the histogram in Fig. 12, then, show some irregularities but these irregularities are not as pronounced as would be expected if many of the parameters of the levels were grossly inaccurate. Although the distribution of the neutron reduced widths follows the general trend of the chi-squared distributions given by Eq. (1) for values of $\nu=1$ and 2, it does not obey either of these distributions exactly. The general trend appears to agree slightly better with the Porter-Thomas distribution than it does with the exponential distribution. However, the exponential and Porter-Thomas distributions differ too little to make a clear choice possible.

[13] C. E. Porter and N. Rosenzweig, Ann. Acad. Sci. Fennieae 44, 1 (1960).

B. Level Spacings

During recent years, a considerable effort has been devoted to trying to establish the shape of the distribution of the individual level spacings relative to the mean for levels of the same spin and parity. (See reference 8 for a list of references to the original papers.) The simplest assumption is that the levels occur completely at random, which leads to an exponential distribution of the form

$$N=k\exp(-\mathcal{S}), \qquad (2)$$

where $\mathcal{S}=S/D$. The quantity S represents the individual level spacing and D the average spacing. The quantity N is the number of spacings per unit interval $\Delta\mathcal{S}$ and k is the total number of spacings. Recently, Wigner[8] proposed a different distribution. He pointed out that if one assumes a random distribution of Hamiltonian matrix elements the levels of the same spin and parity repel each other. The probability that there exists a level at a distance S from a given level is not independent of the distance; for small values of S it is proportional to S. If the same law also holds for large values of S, the probability of finding the next level at a distance S becomes proportional to SdS. On this basis, Wigner surmised that the complete distribution is given approximately by

$$N=k\pi(\tfrac{1}{2}\mathcal{S})\exp(-\tfrac{1}{4}\pi\mathcal{S}^2). \qquad (3)$$

To see whether or not the present data show a repulsion between levels, the observed levels were separated into sequences, each belonging to a given spin and parity, and the mean spacing was computed separately for each sequence. These sequences were then combined into a single group. The combined distribution is shown by the histogram in Fig. 13. For comparison, the theoretical distributions given by Eqs. (2) and (3) are also included in Fig. 13. Although the experimental distribu-

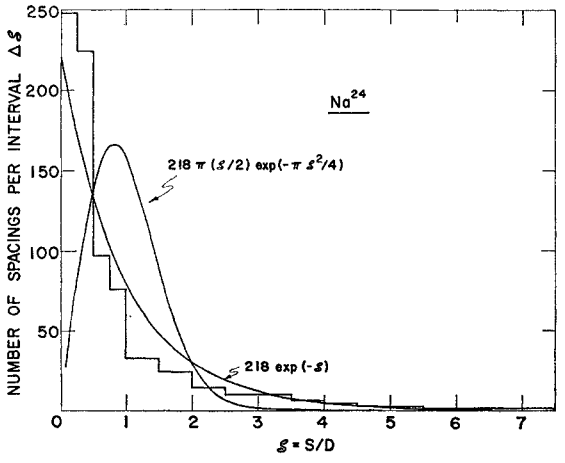

FIG. 13. Distribution of the level spacings of Na^{24}. The histogram shows the data for all virtual levels up to 860 kev. The two curves show the exponential distribution and the distribution given by the Wigner surmise.

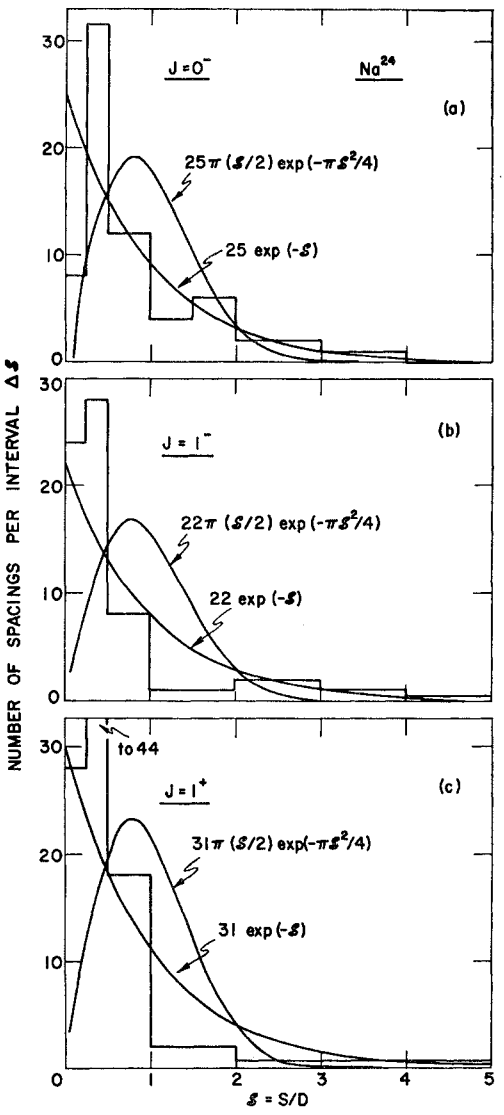

FIG. 14. Distribution of the level spacings of some sequences of Na^{24}. (a) Sequence for $J=0^-$. (b) Sequence for $J=1^-$. (c) Sequence for $J=1^+$. The histograms show the data for the sequences.

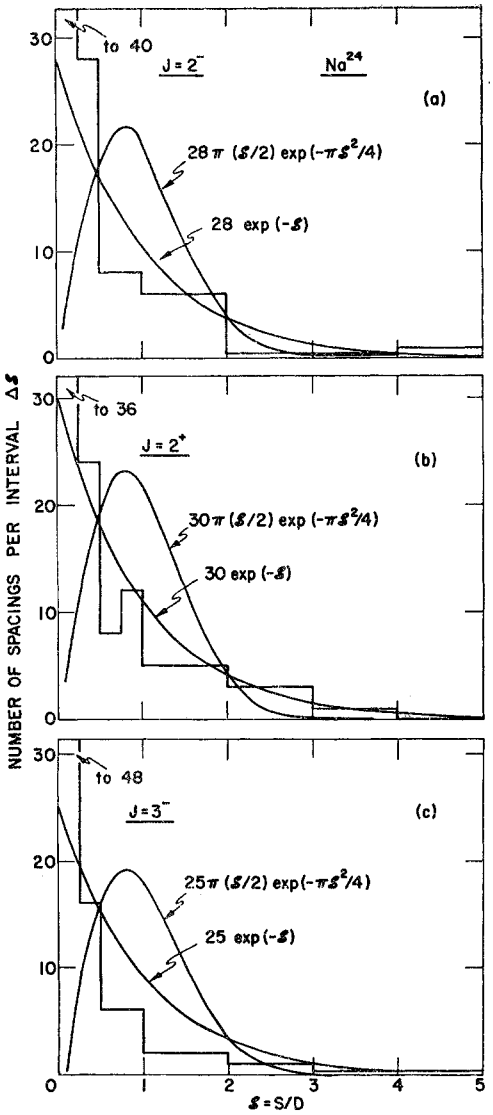

FIG. 15. Distribution of the level spacings of some sequences of Na^{24}. (a) Sequence for $J=2^-$. (b) Sequence for $J=2^+$. (c) Sequence for $J=3^-$. The histograms show the data for the sequences.

tion is not in complete agreement with either theoretical distribution, its general trend is similar to the exponential distribution. The two theoretical distributions differ markedly in their predictions concerning the level spacings. The exponential distribution predicts a large number of small spacings compared with the mean, while the Wigner surmise predicts a small number and a most probable spacing near the mean. The disagreement of the data with the Wigner surmise may have come about because of several reasons: (1) limitations in the experimental method that prevent one from fully resolving the levels, (2) the consequent inaccuracies in the parameters of the levels determined by the analyses, and (3) uncertainties in the values of l. The parameters thus determined may then be equivalent to a somewhat random set. Further, by combining all of the sequences of spacings into a single distribution, one may have introduced an additional random trend among the spacings. To examine this question, a histogram was made for some of the individual sequences. These plots are shown in Figs. 14 and 15. Plots for the exponential distribution and the Wigner surmise are also included with the series of histograms for the appropriate number of spacings. These plots for the individual sequences also show distributions similar to the exponential distribution rather than the Wigner surmise.

C. Angular Momenta

The number of virtual nuclear levels of Na^{24} up to 860 kev is given in Table II for each value of the total

angular momentum J and the distribution among the various values of J is given by the relative numbers. One sees, then, that the values of J range from 0 to 7. In an earlier paper[2] a comparison was made with the theoretical distribution for the levels up to 630 kev. It is desirable now to show the comparison for all values of J up to 860 kev. The expression for the density of levels as a function of the total angular momentum J and the excitation energy U, as derived by Bloch[14] from the single-particle model, is

$$\rho(U,J)=\rho(U)\{\exp[-J^2/2\sigma^2]-\exp\{-(J+1)^2/2\sigma^2]\}, \quad (4)$$

where $\rho(U)$ is the density of all levels and is given by

$$\rho(U)=[\sigma U(96\pi)^{\frac{1}{2}}]^{-1}\exp[\pi(2U/3\delta)^{\frac{1}{2}}], \quad (5)$$

where δ is the average single-particle level spacing of the nucleons. Some authors replace the quantity $2\sigma^2$ by $a\tau$, where τ is the so-called nuclear temperature and a (a constant equal to 3.2 for Na^{24}) can be obtained for any atomic weight by use of an expression given by Cameron.[15] The relative densities of levels for different values of J can be computed by use of Eq. (4). Plots of these relative numbers for various values of σ are shown in Fig. 16. The experimental data for the relative numbers in Table II are shown by solid circles. For comparison, the data[1,2] up to 630 kev are also included and are shown by open circles. The present data indicate a value of $\sigma=2.15$ corresponding to a nuclear temperature of about 2.9 Mev compared with a value of $\sigma=1.8$ and a nuclear temperature of about 2 Mev obtained from the data up to 630 kev. The values of σ and τ up to 630 kev may be closer to the true values than the ones obtained for all of the levels up to 860 kev. Data in the region from 630 to 860 kev cover the region of two clusters of many levels, and a large fraction of these levels exhibit the largest values of J observed in Na^{24}. This introduces a disproportionate number of large values of J into the distribution without including a large number of lower values anticipated at higher energies. The region of energy[16] above 860 kev, as shown in BNL-325, shows that the neutron cross section decreases with energy to comparatively low values. Then, if this region could be included, a large number of low values of J would be expected. Hence, the distribution would shift toward the distribution found for the data up to 630 kev and would lead to lower values of σ and τ than were obtained from all of the data up to 860 kev.

[14] C. Bloch, Phys. Rev. **93**, 1094 (1954). See also H. A. Bethe, Revs. Modern Phys. **9**, 69 (1937); J. M. B. Lang and K. J. LeCouteur, Proc. Phys. Soc. (London) **A67**, 586 (1954); T. D. Newton, Can. J. Phys. **34**, 804 (1956). The expression for $\rho(U,J)$ is sometimes given in the approximate form

$$\rho(U)[(2J+1)/2\sigma^2]\exp[-(J+\tfrac{1}{2})^2/2\sigma^2].$$

[15] A. G. W. Cameron, Can. J. Phys. **37**, 244 (1959).

[16] *Neutron Cross Sections*, compiled by D. J. Hughes and R. B. Schwartz, Brookhaven National Laboratory Report BNL-325 (Superintendent of Documents, U. S. Government Printing Office, Washington, D. C., 1958), 2nd ed.

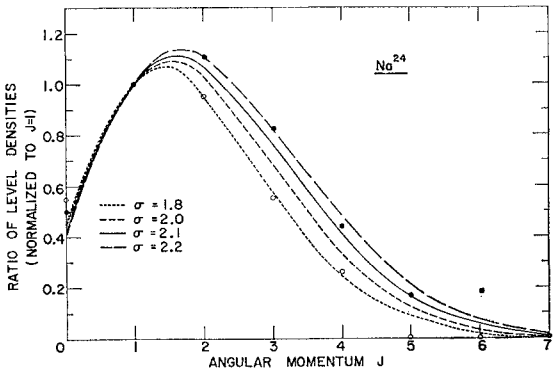

FIG. 16. Distribution of the angular momenta among the resonance levels of Na^{24}. Experimentally determined points are shown by open circles for data up to 630 kev and by solid circles for all of the virtual levels up to 860 kev. The curves are plots of the relative numbers obtained by Eq. (4) for values of $\sigma=1.8$, 2.0, 2.1, and 2.2.

The experimentally determined density of all levels is $\rho(U)=260$ Mev^{-1}. Then, for a mean value of $U=7.4$ Mev and the value of $\sigma=2.15$ obtained from the distribution of the angular momenta, one obtains $\delta\approx0.40$ Mev from Eq. (5), compared with an expected theoretical value[17] of about 0.50 Mev.

D. Strength Functions

The value of the strength function is obtained by the expression $\langle\gamma^2\rangle_{av}/D$, the ratio[2,8] of the average reduced neutron width to the average level spacing, where the reduced neutron width $\gamma_l^2=\Gamma_n/(2P_l)$ and the level spacing are averaged for a given value of l. Up to 630 kev, a value[2] of 0.045 was obtained for the strength function for s-wave levels ($l=0$). Since no additional s-wave levels were identified between 630 and 860 kev, the value of the strength function, if it is to be computed for the entire region up to 860 kev, is reduced to 0.035. No additional p-wave levels ($l=1$) were clearly identifiable between 630 and 860 kev. Then, if this strength function is also to be computed for the entire region up to 860 kev, its value is decreased from 0.37 up to 630 kev to a value of 0.27. However, it should be noted that the p-wave strength function would amount to 0.36 if all levels between 630 and 860 kev were considered to be p-wave levels and combined with the previous p-wave levels up to 630 kev. This comes about because the reduced widths for p-wave levels in this region, as computed from the neutron widths determined by the analysis, are very small. The values of the strength functions for s- and p-wave levels are in agreement with the model proposed by Feshbach *et al.*[18] who predict a maximum for the strength function for p-wave levels and a minimum for s-wave levels in the region of $A=25$ for a nuclear well depth of about 40 Mev. Further, the

[17] A. A. Ross, Phys. Rev. **108**, 720 (1957).

[18] H. Feshbach, C. E. Porter, and V. F. Weisskopf, Phys. Rev. **96**, 448 (1954).

sum rule of Lane *et al.*[4] suggests that the sum of the reduced widths of a given group of levels in an energy interval comparable with the spacings of giant resonances for a given value of l should not exceed $\hbar^2/(\mu R^2)$. The fact that the sum for the p-wave levels is between 0.3 and 0.4 of this limit indicates that the present narrow energy interval is near the maximum for the p-wave strength function. The strength function for d-wave levels ($l=2$) might be expected to be of the same order of magnitude as for s-wave levels since the levels are of even parity. However, up to 630 kev, the strength function for d-wave levels was found to be about 100 times as large as the value for s-wave levels. For the entire energy region up to 860 kev the strength function was found to be 3.9. If all levels from 630 to 860 kev are assumed to be d-wave levels and combined with the levels assigned to $l=2$ below 630 kev, the strength function is 4.5. For the f-wave levels ($l=3$) up to 630 kev, the strength function was found to be 75. For the levels between 630 and 860 kev, it was found to be 57. When all of the levels up to 860 kev were attributed to $l=3$, the strength function was found to be 70. A peak in the value of the strength function for f-wave levels might be expected in the region of the peak for p-wave levels, but it should not be expected to exceed the height for p-wave levels by such a large factor. For the ten levels to which a value of $l=4$ was assigned, the strength function is 60. One, then, sees that reasonable values of the strength functions were obtained for the s- and p-wave levels but excessively large values were obtained for all other values of l. If all of the levels up to 860 kev other than s-wave levels could be considered to be p-wave levels, irrespective of the corresponding values of J, the p-wave strength function turns out to be 0.5 for the neutron widths obtained from the analyses.

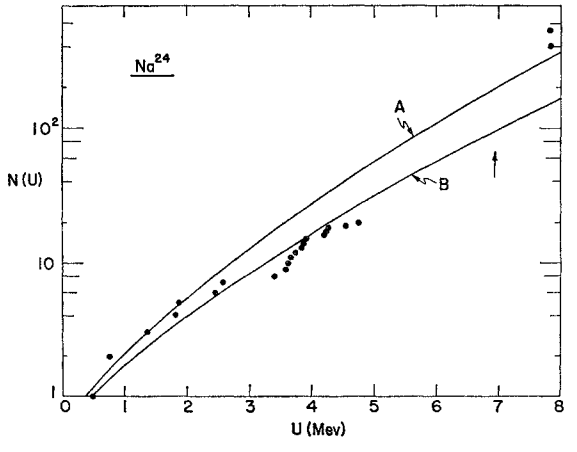

FIG. 17. Distribution of the bound nuclear energy levels of Na^{24} as a function of the excitation energy U. Curve A was obtained from Eq. (6) (times a factor of 1.8) for a value of $\delta=0.50$ Mev and curve B for $\delta=0.60$ Mev. The arrow indicates the binding energy, 6.956 Mev. The two points near 8 Mev were obtained from the neutron resonance levels by use of the two nuclear temperatures discussed in the text.

E. Excited Nuclear Levels

The density of the virtual levels of Na^{24} observed up to 860 kev is large and at first sight appears to be much too large in comparison with the density of the known bound levels. However, only 20 bound levels[19] are known up to about 4.75 Mev and above this energy apparently no measurements have been made. Figure 1 shows a plot of the number of virtual levels with energies $\leqslant E_n$ as a function of the neutron energy E_n for all of the observed levels up to 860 kev. Since only a small fraction of the bound levels have been resolved, it is not known whether or not the plot in Fig. 1 would join on smoothly with a similar plot of the bound levels. One can relate the number of bound levels to the number of virtual levels by an expression for the total number of levels up to an excitation energy U (expressed in the center-of-mass system). The total number of levels in the energy interval from U_1 to U_2 is given by the expression

$$N(U)=\int \rho(U)dU, \tag{6}$$

where $\rho(U)$ is the density of all levels in the energy interval. The theoretical number of levels depends on the form of $\rho(U)$, which is known to have an essentially exponential behavior and a number of expressions have been given for it. The expression given by Bloch,[14] Eq. (5) in the present paper, will be used here. Then the integral, Eq. (6), reduces to the form

$$N(U)=2C\left(\ln x+ax+\frac{a^2x^2}{2\times 2!}+\frac{a^3x^3}{3\times 3!}+\cdots\right), \tag{7}$$

where $x=U^{\frac{1}{2}}$, $C=[\sigma(96\pi)^{\frac{1}{2}}]^{-1}$, and $a=\pi[2/(3\delta)]^{\frac{1}{2}}$. The quantity σ is proportional to the nuclear temperature (assumed to be constant for each nucleus) and δ is the average level spacing of the individual nucleons in the nucleus. Equation (7) cannot include the ground level, whose excitation energy is $U=0$, because of the logarithmic term. However, it was shown previously[2] that the value of $N(U)$ from Eq. (7) is a small negative number when U is as low as 0.10 kev ($\sigma=0.50$ Mev); and therefore the lower limit for U_1 amounts to a small correction. Then, Eq. (7) should reflect the distribution of all excited nuclear levels above the ground level for the proper values of σ and δ. A family of curves for various values of σ and δ, when compared with the experimentally observed levels, can be expected to indicate the proper values of σ and δ for the various nuclei. Many of the bound levels of nuclei have not been resolved as yet but for the ones that have been, the data favor a value of δ of about 0.50 Mev for the odd-odd nuclei in the region of A near 25. About 100 bound levels of Al^{28} have been resolved, so that this nucleus provides

[19] P. M. Endt and C. M. Braams, Revs. Modern Phys. **29**, 683 (1957).

the best means of evaluating δ. (See Fig. 19 of reference 2.) It was pointed out previously[2] that for odd-odd nuclei the curve given by Eq. (7) falls below a plot of the number of bound levels with energies $\leqslant U$ as a function of the excitation energy U for values of δ of 0.50 and 0.60 Mev and that smaller values of δ lead to much steeper curves. However, if the value of $N(U)$ from Eq. (7) is multiplied by a constant of the order of the value of σ, the equation appears to agree with the distribution of the bound levels of odd-odd nuclei (for δ near 0.50 Mev) in the low-energy region where most of the bound levels are known (cf. Figs. 19 and 20 of reference 2).

Figure 17 shows a plot of the known bound levels of Na^{24}. Curves A and B show plots of Eq. (7) (multiplied by 1.8) for $\delta=0.50$ and 0.60 Mev, respectively. Erickson[20] has shown that the number of levels up to an excitation energy U is given by the product of the nuclear temperature and the density of levels, i.e., $N(U)=\tau\rho(U)$. By use of this relation, the two points shown in Fig. 17 by solid circles near 8 Mev were obtained from the neutron resonance levels for nuclear temperatures of 2.0 and 2.9 Mev. These points are near curve A, which corresponds to $\delta=0.50$ Mev.

Figure 18 shows a plot of the known bound levels of two neighboring odd-odd nuclei of Na^{24}, viz., Na^{22} and Al^{26}. This plot shows that the bound levels of these two nuclei also follow the same trend as Na^{24} and Al^{28} (Fig. 19 of reference 2). A number of plots for other odd-odd nuclei all show a similar trend up to 3 or 4 Mev. Above 3 or 4 Mev many of the bound levels apparently have not been resolved. On the basis of the behavior of the bound levels up to a few Mev and the points given by the neutron resonances near 8 Mev, one expects some such curve as A in Figs. 17 and 18 to reflect the shape of the distribution of the nuclear levels for the proper values of σ and δ. One cannot include in Fig. 17 a point for each of the 230 virtual levels of Na^{24}. However, the point shown near 8 Mev in this plot indicates that a much higher percentage of the virtual levels are being located by present techniques than are resolved in the region of the bound levels. Some further observations pertaining to the distribution of the nuclear levels and the behavior of the values of σ and δ are given in reference 2.

6. DISCUSSION

The results show that present counting equipment can achieve a neutron energy spread small enough to see levels having widths comparable with the widths of levels in the low-energy part of the kev region. The results also show that the two large peaks observed by Stelson and Preston[3] in the region between 600 and 850 kev are clusters of levels. A large number of levels were observed all along in the data, even in the wings of the two large peaks and in the valley between them. In this region, the data show no peaks identifiable as s-wave

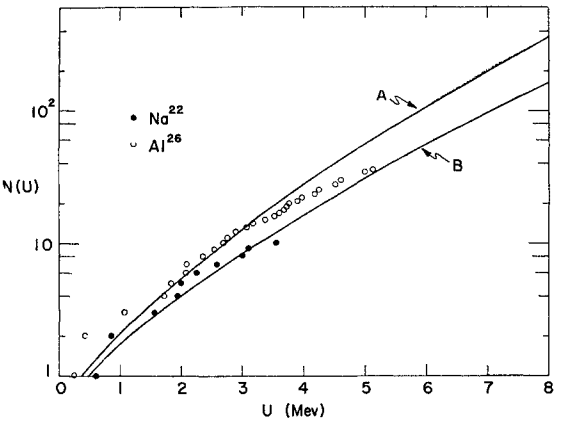

FIG. 18. Distribution of the bound nuclear energy levels as a function of the excitation energy U in two of the odd-odd nuclides adjacent to Na^{24}. Solid circles show the locations of the known bound levels of Na^{22} and open circles the locations of the bound levels of Al^{26}. Curves A and B are explained in the text.

levels. In comparison with the possible theoretical peak heights, the observed peaks are too high for s-wave levels. The nearest approach to the possible heights occurs in the region around 850 kev, where the lowest peak heights were observed. Here, even if one makes the highly unlikely assumption that σ_p is as large as 3.0 b, the observed peak heights of the levels are still well above the possible theoretical heights for s-wave levels. Besides, no deep minima were observed between levels although the level spacing is ample.

An attempt was made to determine the type of levels found in this region. Because of the limitations noted in Secs. 4 and 5, it is not claimed that the parameters were determined with certainty. In order to determine the best possible values of the many parameters, each level was studied by self-detection. The various figures show the lowest minima between peaks and the highest peak values obtained by both flat- and self-detection measurements. Data obtained by self-detection proved to be of considerable help in determining the parameters of the levels. The values of J assigned are the largest that agree with the data by taking into account the wings of overlapping and interfering levels. As previously noted, there appears to be no definite means by which one can distinguish clearly between possible values of l. The analyses show no level with a width greater than 4.10 kev corresponding to a maximum reduced width of 8.9 kev for a p-wave level. Then, if the values of the reduced widths are meaningful, they show a strong preference for values of $l>1$. If all levels are assumed to be attributable to $l=2$, the corresponding reduced widths range from about 30 to 130 kev. One, then, might wish to attribute all levels to d-wave interactions. However, two compelling reasons prevent this assignment: (1) It would conflict with the data because mutual interference would occur for all levels having common values of J. Common values of J are attributable to a

[20] T. Erickson, Nuclear Phys. **11**, 481 (1959).

number of pairs of adjacent levels and to some series of consecutive levels for which no deep minima were observed between levels. (2) One must assign high values of J to a number of levels. For $J=5$, the minimum value of l is 3, for $J=6$, the minimum value is 4, etc. Moreover, the range in the values of l is small for any value of J, being the largest for $J=3$. This range can be further restricted. Because of the very low values of the reduced widths, one assumes that no p-wave levels are present. This removes the value $l=1$ from the ranges of values of l. Then, if one imposes the restriction that only the smallest value of l consistent with the data is to be assigned to each level, no more than two possible values of l for each value of J need be considered. Because of the very large reduced widths corresponding to the large minimum values of l associated with large values of J, some inconsistencies occur. One might try to remove these inconsistencies by one of two methods: (1) Assign the minimum values of l to those levels having high values of J and progressively larger values of l to levels of smaller widths irrespective of the values of J. This method would fail because the reduced widths become excessively large. Further, for small values of J, the upper limit for l is too low. (2) Resolve the wider levels into groups of narrower levels and hence to higher values of l. This would multiply the difficulties because reasonable values of the reduced widths would not occur. Then, for values of $l \geqslant 3$, the sum rule[4] mentioned in the introduction is still violated. In order to avoid this violation, the widths of the levels must be so small that the levels would not have been observed by present techniques. For small values of l, the sum rule and the expressions for the penetrability factors and for the reduced widths appear to be valid; but for larger values of l in the present energy region, there appears to be no means by which one can reconcile these expressions with the data. Further difficulties were also noted in the section on strength functions. Values of the strength function obtained for s- and p-wave levels appear to be reasonable and are in accord with the predictions of theory.[18] For larger values of l, very large values of the strength functions were found because the reduced widths become excessive.

Apropos the large values of the reduced widths for large l, Lane[21] has recently evaluated the reduced widths for many levels. In Table XIII of his report, reduced widths were evaluated for two values of l for one level of Na^{24} and his value of the reduced width for $l=2$ exceeds by a factor of 10 the value for $l=1$.

The differential neutron cross-section measurements made by Lane and Monahan[22] in the vicinity of the two large peaks near 710 and 790 kev observed by Stelson and Preston[3] are not inconsistent with a high density of levels and large values of l. Their results indicate a considerable amount of interference between levels of opposite parity. They see more evidence of resonance structure corresponding to high values of l in the region of the second large peak near 790 kev than in the region of the first large peak. This is because of their large neutron energy spread of about 25 kev and the distribution and type of levels which form the two large clusters of peaks. The present data show the presence of two similar relatively wide levels near the peak of the cluster near 780 kev, whereas in the first cluster, which shows a peak near 710 kev, the level spacing is larger for relatively wide levels.

ACKNOWLEDGMENTS

I wish to express my appreciation to Dr. F. E. Throw for his comments and suggestions with the manuscript, to Dr. G. R. Ringo for his comments and suggestions, and to Dr. J. E. Monahan and Dr. Norbert Rosenzweig for their helpful discussions. I wish also to express my thanks to Jack Wallace, William Evans, and the Van de Graaff crew for their aid in taking the data. The author also wishes to thank the Applied Mathematics Division for much of the detailed computations.

[21] A. M. Lane, Revs. Modern Phys. **32**, 519 (1960).
[22] R. O. Lane and J. E. Monahan, Phys. Rev. **118**, 533 (1960).